ELSEVIER

Wear 176 (1994) 231–237

WEAR

Modelling friction and wear of scratching ceramic particle-reinforced metal composites

Zhenfang Zhang, Liangchi Zhang, Yiu-Wing Mai*

Centre for Advanced Materials Technology, Department of Mechanical and Mechatronic Engineering, University of Sydney, Sydney, NSW 2006, Australia

Received 11 January 1994; accepted 21 April 1994

Abstract

The friction and wear behaviour of 6061 aluminium matrix composites reinforced with SiC and Al_2O_3 particles has been investigated at relatively high loads and speeds on a conventional scratch machine using a pyramidal indenter. It is identified that ploughing, adhesion and particle fracture all contribute to the friction and wear. The friction coefficient increases with particle volume fraction but is independent of the range of normal loads (1–20 N) and sliding speeds (1–10 mm s^{-1}) tested. The wear volume generally increases with normal load and sliding distance (or pass number), and decreases with increasing particle volume fraction. A comparison of the measured scratch hardness and Vickers hardness shows that the former is not simply proportional to the latter for composites reinforced with large particles. A new friction and wear model is then established based on the theories of adhesion and ploughing and the effect of particle fracture. The validity of the model is confirmed by experiments and microscopic observations on the scratch topography of the metal matrix composites.

Keywords: Ceramics; Composites; Al_2O_3; Scratch test; Friction; Wear

1. Introduction

In a wear system, because of unavoidable roughness of the two mating surfaces which give rise to the multiple-asperity contact phenomenon, the real contact area is much smaller than the nominal area. To understand the inherent mechanisms of this complex wearing process, experiments of sliding a single point indenter on a target material have been conducted by many researchers [1–7]. The removal of material caused by hard abrasives is called abrasive wear or abrasion. It has been found that the abrasion is a main form of wear in metals [1] and composites [8,9], and the groove formation is important to understand wear mechanisms [2,10]. A simple expression for the volume of material removed during two-body abrasion by a conical abrasive is given by [3]

$$\frac{W_v}{S} = \frac{2\tan\alpha}{\pi}\frac{P}{H} \tag{1}$$

where W_v is the volume loss due to wear, S the sliding distance, P the normal load on the conical abrasive, H the hardness of the wearing surface and α the attack angle of the abrasive particle. Replacing the factor $(2\tan\alpha)/\pi$ by a wear coefficient K, the well-known Archard's wear law

$$\frac{W_v}{S} = K\frac{P}{H} \tag{2}$$

is obtained. This model is generally true for most single-phase metals. However, there are two observations that are inconsistent with Archard's equation: (1) an abrupt change in wear rate can sometimes be found if the pressure or sliding velocity is changed; and (2) the wear rate can increase with increasing hardness, if the attack angle of the abrasive particle varies or the material has a low fracture toughness [11,12]. A modification of Archard's equation was proposed by Hornbogen [12] to include fracture toughness effects of some metallic materials when the applied strain exceeded the critical fracture strain. However, these wear models have never been related to the role of a second-phase particle in a composite material. A fixed-depth scratch on Al–Si

*On leave at the Department of Mechanical Engineering, Hong Kong University of Science and Technology, Clear Water Bay, Hong Kong.

SSDI 0043-1648(94)06463-R

alloy [10] showed that fracture of ceramic particles occurred and controlled the wear mechanisms. Indentation on monolithic brittle materials [13,14] also indicated that fracture of the material might influence wear significantly, and Lawn [9] proposed a wear model for brittle solids under fixed abrasive conditions. The model has a form similar to Archard's wear equation. Evans and Wilshaw [14] pointed out that material removal by abrasive wear was due to the lateral cracks spreading to the material surface and they proposed another wear model which contains both the fracture toughness and the hardness of the material. The effect of sliding friction force on the strength of brittle materials was also studied [8] and it was concluded that, although frictional effect plays a relatively minor role in strength degradation, the threshold condition for cracking is sensitive to the level of friction.

Bowden and Tabor [4] suggested that the friction coefficient μ was caused by the combination of adhesion μ_a and ploughing μ_p:

$$\mu = \mu_a + \mu_p \quad (3)$$

Following this theory, much attention has been paid to study the adhesion and ploughing effects on the frictional force. Some models of friction and wear have been proposed [1,6,7] and proved to be useful for most metals. Unfortunately, those models concerned only the hardness of the wearing material and the geometry of the abrasive particle. The important effect of the particle reinforcement in metal matrix composites has never been fully understood. It is therefore the purpose of the present paper to make a careful investigation on the scratch behaviour of aluminum matrix composites reinforced with ceramic particles and to establish a theoretical model to explain these phenomena.

2. Experimental work

Wear tests were carried out on a scratch wear machine. A detailed description of the experimental method has been reported elsewhere [15]. For the present work, a pyramidal indenter with an apex angle 2θ of 136° was used and the orientation of the indenter was taken with one leading plane moving forward during scratching. A range of linear velocities of 1–10 mm s^{-1} was used over a wear track about 6 mm long. The normal load was varied from 1 to 20 N.

The tangential forces were measured using an LVDT and recorded by a computer. The average value of the tangential force for each scratch was taken from at least eight experimental points and each test condition was repeated three times. The friction coefficient is defined by $f = F_t/P$, where F_t is the tangential force and P the applied normal load on the indenter.

The samples were 6061Al-matrix reinforced with 10 vol.% and 20 vol.% acute-shaped SiC particles with an average diameter of 1.8 μm, and 10 vol.% and 20 vol.% acute-shaped alumina (Al_2O_3) particles with average diameters of 4.5 μm (for 10 vol.%) and 8.8 μm (for 20 vol.%), supplied by Comalco Pty Ltd, Australia. All the composites underwent the same T6 heat treatment, i.e. 1.5 h solution treatment at 530 °C, quenching into water followed by natural aging for 20 h and then artificial aging at 175 °C for 8 h. Disk-shape specimens were polished down to 1 μm using diamond paste and cleansed with acetone prior to the scratch test.

3. Results and discussion

3.1. Groove formation and definition of cross-sectional area

The bulk composite material was first plastically deformed under static indentation. The indenter was then moved forward under the same normal load. A V-shaped groove, which was almost identical with the pyramidal geometry, was formed on the specimen surface. This V-shaped groove profile was observed with the aid of the laser confocal image method, as shown in Fig. 1. The groove depth increased with increasing applied load. In the load range studied here, the groove dimensions were much larger than the particle sizes and V-shape grooves with uniform cross-sections were always obtained, even at the smallest load level of 1 N. Microscopic observations demonstrated that the indenter would rise only slightly when it scratched through very large particles and fractured them. However, the magnitude of such a movement was so small that its influence on the total wear volume was negligible. Therefore, the groove size in this study could be considered as a constant in a sliding pass. Fig. 2 shows the groove shape of (a) 10% SiC–Al composite and

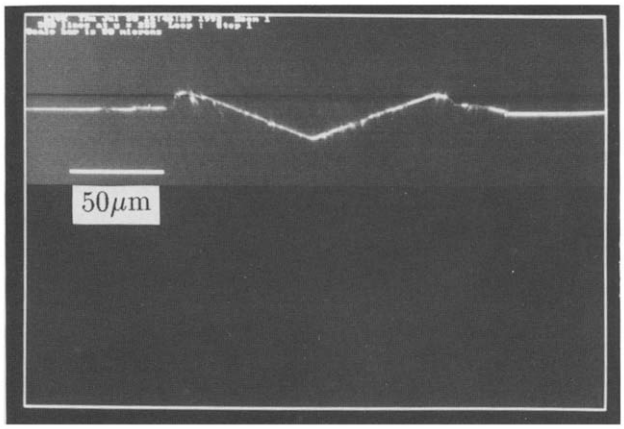

Fig. 1. Laser confocal image showing the groove shape of 20 vol.% Al_2O_3–Al composite under a normal load of 12 N.

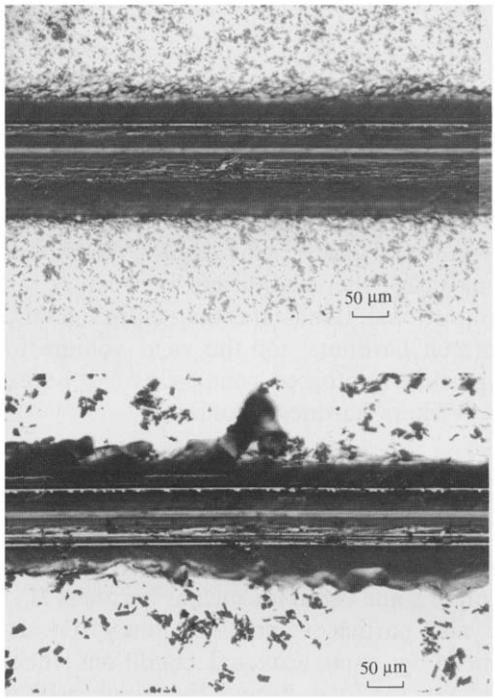

Fig. 2. Groove shape at a normal load of 9 N: (a) 10 vol.% SiC–Al composite; (b) 10 vol.% Al_2O_3–Al composite.

(b) 10% Al_2O_3–Al composite, at a normal load of 9 N.

Because of the sharp edge of the indenter, some cutting could also be found. A prow was formed ahead of the indenter and the material was continually displaced sideways to form ridges adjacent to the groove. However, the grooves showed a slight difference for different types of reinforced composites. For example, the composite with 20 vol.% Al_2O_3 particles results in shallower groove depth and rougher ridges than those with 10 vol.% SiC particles. The reasons are that the hardness of the former is higher than that of the latter and that larger particle reinforcement is likely to be fractured. In the ideal case of ductile metals, ploughing due to a single pass of scratch does not result in any material detachment from a worn surface [1]. However, since the present composites are relatively brittle, the majority of the ridges (i.e. materials displaced sideways) are fractured. These loose ridges have a very small load-carrying capacity and hence are easily removed by the ensuing passes during repeated wear. It is therefore reasonable to define in the present study that the effective cross-sectional area A_p is equal to the area of the groove inside the original surface of the composite, as shown in Fig. 3, i.e. $A_p = wd/2$, where w is the width and d is the depth of the groove.

3.2. Scratch mechanisms

Ploughing is a dominant scratch mechanism for many ductile materials and can be proved by the groove

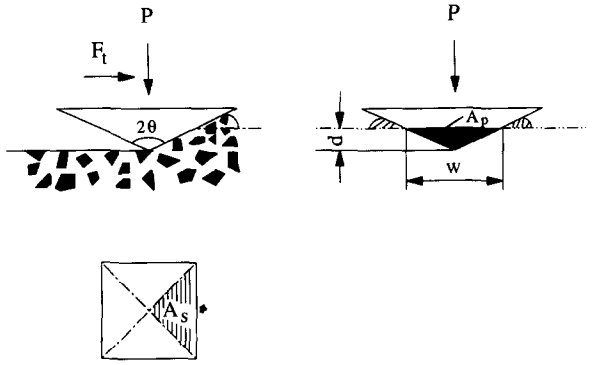

Fig. 3. Configuration of the scratch by a pyramidal indenter.

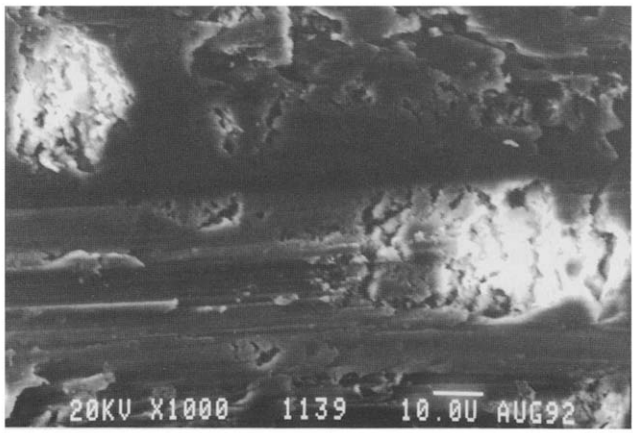

Fig. 4. Scanning electron micrograph showing fractured Al_2O_3 particles under a normal load of 9 N.

topography. However, there are some important factors that should be specially taken into account for these metal matrix composites reinforced with ceramic particles. For instance, fractured particles could always be observed on the groove surface in our tests loaded from 1 to 20 N. Most particles on the scratch path were fragmented by the indenter. This fracture phenomenon became severe for Al_2O_3-reinforced composites, because the reinforced particle size was large, as shown in Fig. 4. It indicated that the particles would hinder the forward movement of the indenter until they were fractured. In other words, a force is needed to fracture these particles. Fig. 4 also shows good adhesion between the contact surfaces during scratching and it contributes to the frictional force as well. It therefore follows that the mechanisms for scratching the present composites consist of three components: (1) ploughing of the composite; (2) adhesion between the counterfaces; and (3) fracture of the particles. All of them contribute to the macroscopic frictional force.

3.3. Vickers hardness and scratch hardness

Vickers hardness has been used as a main material parameter in many wear models for single-phase metals [1,3,4]. However, it has been questioned if the wear

rate of a multi-phase composite could also be related to this parameter simply by Eq. (2). Conversely, the scratch hardness has been introduced in some related studies [6,16,17], although there is no standard measurement method for it. It is therefore necessary to understand the difference between these two hardness measurements before any practical modelling is made.

First, we recall the definition of the Vickers indentation hardness, which is obtained by dividing the applied normal load P by the surface area of the indentation A_1:

$$H_v = \frac{P}{A_1} = \frac{2P\sin(2\theta)}{d_1^2} \quad (\text{kgf mm}^{-2}) \tag{4}$$

where d_1 is the mean diagonal of the indentation.

The Vickers hardness was measured for all the composites investigated under normal loads from 25 to 1500 gf (i.e. 0.25–15 N). The average value was obtained from five measurements at each load level. As shown in Fig. 5, the H_v values are almost constant over the whole range of applied loads for the SiC–Al composites, but for the Al_2O_3–Al composites these values increase slightly with increasing load for loads less then 1 N and remain constant for larger loads. For realistic measurements of the Vickers hardness for different particle-reinforced composites investigated in this work, therefore, an indentation load of 5 N was applied throughout.

Now consider the scratch hardness, which is the ratio of the normal load P on the indenter to the projected contact area of the horizontal plane A_p [16], as shown in Fig. 3. In the present investigation, it is also assumed that only the leading edge of the indenter contact the test material [6]. The scratch hardness, H_s is then given by

$$H_s = \frac{P}{A_s} = \frac{4P}{w^2} \tag{5}$$

where w is already defined as the groove width. Then the cross-sectional area A_p is

$$A_p = A_s \cot\theta = \cot\theta \frac{P}{H_s} \tag{6}$$

A comparison of the scratch hardness with Vickers hardness versus normal load is presented in Fig. 5. For SiC–Al composites containing very small reinforcing particles, they follow approximately a linear relationship of $H_s = 5.3\ H_v$. However, for Al_2O_3–Al composites with large particles, the relationship between H_v and H_s is not proportional. It indicates that, unlike metals, neither the scratch hardness nor the wear volume for those large particle-reinforced composites can be expressed by the Vickers hardness alone.

3.4. The cross-sectional area

The cross-sectional area of a scratch is a strong function of some variables such as hardness H_v, particle size a and particle volume fraction f_v [1]. It is also influenced by some external conditions such as the applied normal load P, and the number of passes n of a scratch test.

The cross-sectional areas decrease generally with increasing Vickers hardness, but does not necessarily follow a linear relationship as indicated in Fig. 6. This presents some slight differences from the observations on metals [1,17]. Fig. 7 shows a linear relationship between the cross-sectional area and the number of passes and implies that the wear volume would be proportional to the sliding distance in a real wear situation. For the present case of a single-pass scratch, the cross-sectional area is almost constant along the groove so that the wear volume is a product of the cross-sectional area and the sliding distance. In Fig. 8, the solid symbols which are obtained from the scratch tests show that the cross-sectional areas increase linearly with increasing normal load for the Al_2O_3–Al composites.

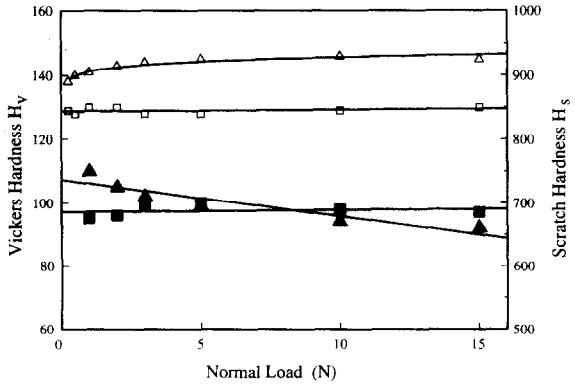

Fig. 5. Variation of Vickers hardness H_v (open symbols) and scratch hardness H_s (full symbols) with normal load P for 10 vol.% SiC–Al (□, ■) and 20 vol.% Al_2O_3–Al (△, ▲) composites.

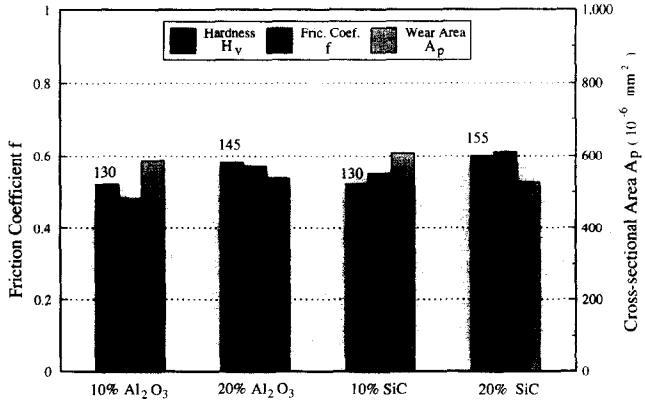

Fig. 6. Vickers hardness H_v, friction coefficient f and cross-sectional area A_p under a normal load of 9 N for different SiC–Al and Al_2O_3–Al composites.

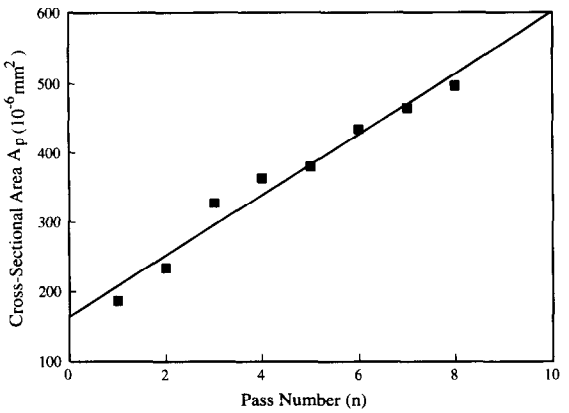

Fig. 7. The relationship between cross-sectional area A_p and pass number n under a normal load of 2.5 N for the 20 vol.% Al_2O_3–Al composite.

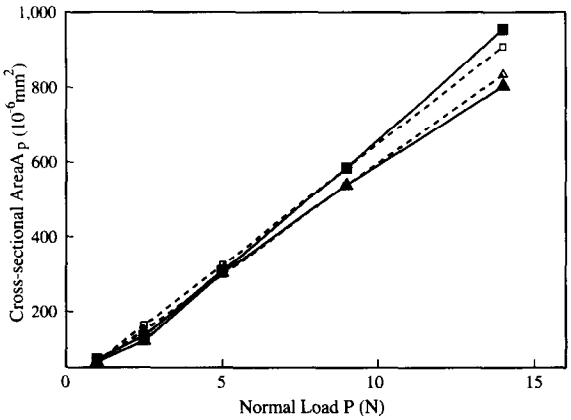

Fig. 8. Experimental data and predicted cross-sectional areas for Al_2O_3–Al composites. (Experiment: ■, 10 vol.%; ▲, 20 vol.%. Theory: □, 10 vol.%; △, 20 vol.%).

In addition, scratch tests under different sliding velocities from 1 to 10 mm s^{-1} were carried out for 10 vol.% SiC–Al and 20 vol.% Al_2O_3–Al composites. No significant changes of friction coefficient and wear volume were found. Therefore, the effect of sliding speed on the wear volume and friction coefficient is negligible in these two composites.

Generally speaking, higher particle volume fraction results in higher hardness, and both bring about lower wear volume (or cross-sectional area). Unfortunately, no apparent relationship is available so far to correlate the friction and wear behaviour with these parameters. This consideration is elucidated in the following section.

4. A new theoretical model

As has been discussed before, in addition to the components of adhesion and ploughing, particle fracture also plays an important role in making up the total frictional force. Hence, the overall frictional force should be given by

$$F_t = F_a + F_p + F_f \tag{7}$$

where F_a, F_p and F_f are the components caused by adhesion, ploughing and particle fracture, respectively. To calculate these individual frictional forces, the following assumptions are made based on experimental observations: (a) there is no particle debonding; (b) particles are uniformly distributed and have an average size a; and (c) the diamond indenter is rigid.

If the shear strength at the interface between the composite and indenter is s, and the flow or yield pressure is p, the adhesion and ploughing force will be

$$F_a = sA_s = sA_p \tan\theta \tag{8}$$

and

$$F_p = pA_p \tag{9}$$

Plasticity theory shows that the shear or yield strength of a material is proportional to its hardness. This is assumed to be true for the present bulk material. Thus the combination of the adhesion and the ploughing parts can be expressed in terms of the Vickers hardness:

$$F_a + F_p = (s \tan\theta + p)A_p = k_1 A_p H_v \tag{10}$$

where k_1 is a geometric factor. In the above equation, the frictional force caused by the particle is not included.

The contribution of the particle fracture to the frictional force can be derived from the Griffith equation [18], which leads to the fracture stress of a hard particle as

$$\sigma_f = c_1 \frac{K_{1c}}{a^{1/2}} \tag{11}$$

where c_1 is a constant, K_{1c} is the fracture toughness of the composite and a is the particle size which is considered to be proportional to the crack size. The stress on the particle applied by a pyramidal indenter can be determined by

$$\sigma = c_2 \frac{F_f}{f_v A_p} \tag{12}$$

where c_2 is a geometric factor and f_v is the particle volume fraction.

Combining Eqs. (11) and (12) gives

$$F_f = k_2 A_p f_v \frac{K_{1c}}{a^{1/2}} \tag{13}$$

where $k_2 = c_1/c_2$ being a geometric factor for the particle-reinforced composites. The sliding friction coefficient f is then given by

$$f = \frac{F_a + F_p + F_f}{P} \tag{14}$$

Substituting Eqs. (10) and (13) into Eq. (14) gives a straightforward expression for the cross-sectional area A_p as

$$A_p = \frac{fP}{k_1 H_v + k_2 f_v \frac{K_{1c}}{a_{1/2}} \times 100} \quad (\mathrm{mm}^2) \tag{15}$$

where k_1 and k_2 can be determined from two sets of experimental data for any given composite. For example, for the Al_2O_3–Al composites, it is found that $k_1 = 13.8$ and $k_2 = 49$ when the following data are used: (1) for 10 vol.% Al_2O_3–Al composite: $f = 0.48$, $P = 9$ N, $H_v = 130$ kgf mm^{-2}, $f_v = 0.1$, $a = 4.5$ μm, $K_{1c} = 24.2$ MPa m$^{-1/2}$ and $A_p = 585 \times 10^{-6}$ mm^2; and (2) for 20 vol.% Al_2O_3–Al composite: $f = 0.57$, $P = 9$ N, $H_v = 145$ kgf mm^{-2}, $f_v = 0.2$, $a = 8.8$ μm, $K_{1c} = 22.8$ MPa m$^{1/2}$ and $A_p = 538 \times 10^{-6}$ mm^2, where K_{1c} values are taken from [19].

Fig. 8 shows both experimental data and predicted cross-sectional areas from Eq. (15) for Al_2O_3 particle-reinforced aluminum composites under different loads. The good agreement achieved between theory and experiments has confirmed the validity of the proposed wear model.

The wear volume V for a single scratch can also be predicted:

$$V = A_p L = \frac{fLP}{k_1 H_v + k_2 f_v \frac{K_{1c}}{a^{1/2}} \times 100} \quad (\mathrm{mm}^3) \tag{16}$$

where L is the sliding distance in mm. At first appearance, the wear volume increases proportionally with the increase of the normal load, sliding distance and friction coefficient, but decreases with increasing Vickers hardness, particle volume fraction and the ratio $K_{1c}/a^{1/2}$. Unlike previous models, Eq. (16) reveals that many variables influence the wear volume. The advantage of the present model is that it involves the most important properties of the wearing materials in a simple expression and describes explicitly their correlations.

5. Conclusions

Based on observations of the scratch test, the mechanisms of single-point scratching have been identified as the abrasion of the composite, adhesion between the contact surfaces and the fracture of the reinforced particles. These three parts all contribute simultaneously to the friction and wear behaviour of the composite. A new theoretical model has been proposed to explain the friction and wear behaviour of the metal matrix composites studied. The test results indicate good agreement with the theoretical predictions on the Al_2O_3–Al composites with large particles. The model does not include interactions between many abrasive particles acting simultaneously, but this could be conducted if the number and spacing of the abrasives are known.

Acknowledgments

The authors wish to thank the Australian Research Council for the support of this work and Comalco Research Centre in Melbourne for supplying the metal matrix composites for testing. The Sydney University Electron Microscope Unit has kindly provided access to its facilities. Z.F. Zhang is supported by an EMSS scholarship.

References

[1] K.H. Zum Gahr, *Microstructure and Wear of Materials, Tribology Series*, Vol. 10, Elsevier, Amsterdam, 1987.
[2] M.A. Moore and F.S. King, Abrasive wear of brittle solids, *Wear, 60* (1980) 123–140.
[3] E. Rabinowicz, *Friction and Wear of Materials*, Wiley, New York, 1965.
[4] F.P. Bowden and D. Tabor, *The Friction and Lubrication of Solids*, Vols. I and II, Clarendon Press, Oxford, 1954, Oxford Univ. Press, Oxford, 1964.
[5] J. Goddard and H. Wilman, A theory of friction and wear during the abrasion of metals, *Wear, 5* (1962) 114–135.
[6] T. Hisakado, On the mechanism of contact between solid surfaces, *Bull. JSME, 13* (1970) 129–139.
[7] A.J. Sedriks and T.O. Mulhearn, Mechanics of cutting and rubbing in simulated abrasive process, *Wear, 6* (1963) 457–466.
[8] B.R. Lawn, S.M. Wiederhorn and D.E. Roberts, Effect of sliding friction forces on the strength of brittle materials, *J. Mater. Sci., 19* (1984) 2561–2569.
[9] B.R. Lawn, A model for the wear of brittle solids under fixed abrasive conditions, *Wear, 33* (1975) 369–372.
[10] S.V. Prasad, P.K. Rohatgi and T.H. Kosel, Mechanisms of material removal during low stress and high stress abrasion of aluminum alloy–zircon particle composites, *Mater. Sci. Eng., 80* (1986) 213–220.
[11] M.M. Khruschov, Principles of abrasive wear, *Wear, 28* (1974) 199–214.
[12] E. Hornbogen, The role of fracture toughness in the wear of metals, *Wear, 33* (1975) 251–159.
[13] B.R. Lawn and T.R. Wilshaw, Review Indentation fracture: Principles and applications, *J. Mater. Sci., 10* (1975) 1049–1081.
[14] A.G. Evans and T.R. Wilshaw, Quasi-static solid particle damage in brittle solids: Observations, analysis and implications, *Acta Metall., 24* (1976) 939–956.
[15] Z.F. Zhang, Y.X. Chen, A.K. Mukhopadhyay and Y.W. Mai, Friction and wear of 6061 Al reinforced with ceramic particulate at elevated temperature, *MMC-3, Proc. 3rd Australian Forum on Metal Matrix Composites, 1992*, pp. 63–73.

[16] C.A. Brookes, P. Green, P.H. Harrison and B. Moxley, Some observations on scratch and indentation hardness measurements, *J. Phys. D: Appl. Phys., 5* (1972) 1284–1293.
[17] T.A. Adler and R.P. Walters, Wear and scratch hardness of 304 stainless steel investigated with a single scratch test, *Wear, 162–164* (1993) 713–720.
[18] S.J. Sharp, M.F. Ashby and N.A. Fleck, Material response under static and sliding indentation loads, *Acta Metall. Mater., 41* (1993) 685–692.
[19] M.J. Hadianfard, J.C. Healy and Y.-W. Mai, Fracture toughness of discontinuously reinforced aluminium 6061 matrix composites, *J. Mater. Sci., 28* (1993) 6217–6221.